# Exploring Methods for MRI Artifact Correction: A Scoping Review

# Exploración de métodos para la corrección de artefactos en resonancia magnética: una revisión del alcance

**Ríos-Pérez Jesús D.[1], Sánchez-Torres German [2], Branch-Bedoya John W. [3]**
[1] MSc(c), Student, National University of Colombia, Grupo de investigación y desarrollo en Inteligencia Artificial, Medellín, Antioquia, Colombia.
[2] PhD, Professor, University of Magdalena, Grupo de Investigación y Desarrollo en Sistemas y Computación, GIDSYC, Santa Marta, Magdalena, Colombia.
[3] PhD, Professor, National University of Colombia, Grupo de investigación y desarrollo en Inteligencia Artificial, Medellín, Antioquia, Colombia.
Correspondence: jriospe@unal.edu.co

Cite this article as: J. Ríos-Pérez, G. Sánchez-Torres, John W. Branch-Bedoya, "*Exploring Methods for MRI Artifact Correction: A Scoping Review",* Prospectiva, Vol 24, N° 1, 2026.

**Recibido: 26/10/2025 / Aceptado: 13/12/2025**

*http://doi.org/* 10.15665/rp.v24i1.3853

## ABSTRACT

Artifact correction in magnetic resonance imaging (MRI) spans from acquisition/reconstruction and hardware strategies to rapidly evolving deep learning (DL) approaches. We conducted a PRISMA-ScR–aligned scoping review to map what is corrected, how it is evaluated, and where evidence gaps persist. PubMed and Scopus were searched over the last five years and complemented by hand-searching. For each record we charted artifact family, MRI sequence and field strength, data source (real vs. simulated), method class, evaluation metrics, and code/data availability. The core synthesis comprises 16 MRI studies: 11 MRI+DL investigations (dominated by U-Net variants with some recurrent/transformer models) and 5 traditional or hybrid MRI techniques (e.g., motion-robust acquisitions, metal-artifact reduction). Two additional DL papers in related modalities were retained as context only to discuss transferability and were excluded from counts, tables, and metrics. DL methods show strong gains in targeted scenarios, while traditional techniques remain reliable baselines. However, heterogeneity in datasets and protocols, scarce multicenter validation, and the lack of open, task-standardized benchmarks limit comparability and clinical generalizability.

**Keywords:** artifact, MRI, deep learning, image correction, UNet, CNN.

**RESUMEN**

La corrección de artefactos en imágenes por resonancia magnética (MRI) abarca desde estrategias de hardware y de adquisición/reconstrucción hasta enfoques de aprendizaje profundo (DL) en rápida evolución. Realizamos una revisión de alcance alineada con PRISMA-ScR para mapear qué se corrige, cómo se evalúa y dónde persisten las brechas de evidencia. Se buscaron estudios en PubMed y Scopus durante los últimos cinco años y se complementó con búsqueda manual. Para cada registro se extrajeron la familia de artefacto, la secuencia y el campo de MRI, la fuente de datos (reales vs. simulados), la clase de método, las métricas de evaluación y la disponibilidad de código/datos. La síntesis central comprende 16 estudios MRI: 11 investigaciones MRI+DL (dominadas por variantes de U-Net, con algunos modelos recurrentes o basados en transformadores) y 5 técnicas tradicionales o híbridas (p. ej., adquisiciones robustas al movimiento y reducción de artefactos por metal). Dos artículos adicionales de DL en modalidades afines se retuvieron solo como contexto para discutir transferibilidad y se excluyeron de conteos, tablas y métricas. Los métodos DL muestran ganancias sólidas en escenarios específicos, mientras que las técnicas tradicionales siguen siendo líneas base confiables. Sin embargo, la heterogeneidad de conjuntos de datos y protocolos, la escasa validación multicéntrica y la ausencia de benchmarks abiertos y estandarizados limitan la comparabilidad y la generalización clínica.

**Palabras claves:** artefactos, imágenes de resonancia magnética, aprendizaje profundo de máquina, corrección de imágenes, UNet, CNN.

## 1. INTRODUCTION

Magnetic resonance imaging (MRI) has become a fundamental tool for medical diagnostics, offering non-invasive imaging capabilities across a wide range of clinical applications [1]. Its versatility—from cardiovascular imaging to neurological evaluations—makes MRI indispensable in current clinical practice. However, the inherent complexity of MR physics and physiology frequently leads to image artifacts that can compromise diagnostic accuracy [2].

Artifact correction in MRI is challenged by diverse clinical scenarios. In cardiovascular MRI, thoracic anatomy together with cardiac/respiratory motion and rapid blood flow produce motion- and flow-related artifacts [2]. In pediatric imaging, long acquisitions and motion artifacts complicate diagnostic quality, sometimes necessitating sedation or general anesthesia with additional clinical risks and operational impact [1]. In MR neurography, maintaining signal-to-noise ratio (SNR) while preserving spatial resolution remains difficult—particularly with acceleration techniques that can amplify noise [3]. In neurological and musculoskeletal contexts, magnetic susceptibility artifacts—especially with metallic implants—degrade diagnostic quality and often require specialized mitigation strategies [4]. Despite advances in acceleration and reconstruction, sustaining diagnostic quality while reducing scan time remains a persistent challenge [1]. These limitations are accentuated in specialized settings such as deep brain stimulation (DBS) imaging and low-field MRI, where parameter optimization and artifact correction are even more complex [5,6]. In cardiovascular applications, balancing temporal resolution with spatial precision continues to be critical [2].

Beyond application-specific issues, there are technical challenges to implementing effective correction strategies. In deep learning (DL)–based reconstruction, a common obstacle is the limited availability or access to large, well-curated datasets for training and validation [6]. Moreover, advanced correction pipelines must balance image quality, reconstruction time, and clinical feasibility. Standardizing techniques across MRI platforms and field strengths remains difficult [7], and cross-study comparability is further constrained by heterogeneous protocols, datasets, and metrics.

Recent studies have reported advances in treating MRI artifacts across clinical domains. In cardiovascular imaging, several works mitigate motion-related artifacts and sequence-specific distortions [2]. DL-based reconstructions have shown improvements in image quality and reader confidence, with notable gains also reported in neurography [3] and in standardized quality-assurance efforts tailored to specific sequences [7]. In post-arthroplasty imaging, metal-artifact-reduction strategies have enabled substantially improved visualization [4]. Collectively, these developments suggest complementary roles for traditional and DL-based approaches, each effective within their intended regimes.

Despite recent advances, most solutions remain artifact-specific and lack multicenter validation. We therefore conduct a PRISMA-ScR–guided scoping review to map MRI artifact-correction methods (acquisition, reconstruction, post-processing), describe datasets and metrics, and identify evidence gaps for future clinical translation. Non-MRI studies are reported only as context-only and excluded from the core synthesis. Despite this progress, important gaps persist. Many solutions target a single artifact type, and few frameworks address multiple artifacts in a unified manner. Figure 1 illustrates representative imaging artifacts (primarily MRI). Standardization across acquisition protocols, reconstruction procedures, platforms, and field strengths remains limited [7]. These gaps motivate a scoping review to map methods, summarize how they are evaluated, and identify areas needing stronger evidence.

Based on the above, the research question that guided this review is: Which techniques, methods, and models have been reported for MRI artifact correction, which artifact types and MRI settings do they address, how are they evaluated (datasets and metrics), and what gaps remain for future research and clinical translation?

We conducted a scoping review following PRISMA-ScR guidance. We searched Scopus and PubMed over the last five years and complemented database results with hand-searching. Eligible studies were charted by artifact type, MRI sequence and field strength, data characteristics (real vs. simulated), method family, metrics, and code/data availability, and synthesized narratively.

Figure 1. Representative artifacts. (a) Motion blur/ghosting in axial brain MRI. (b) Metal streaks / beam hardening in chest CT (non-MRI example, context only). (c) Rotational motion ghosting and blurring in brain MRI. (d) Zipper artifact (RF interference/“spike” in k-space) in spine MRI. (e) Magnetic susceptibility with EPI distortion and signal dropout in diffusion/ADC MRI (skull base).

Figura 1. Artefactos representativos. (a) Desenfoque/ghosting por movimiento en RM cerebral axial. (b) Estrías por metal / beam-hardening en TC torácica (ejemplo no-RM, solo contextual). (c) Ghosting y borrosidad por movimiento rotacional en RM cerebral. (d) Artefacto zipper (interferencia RF/“spike” en k-espacio) en RM de columna. (e) Susceptibilidad magnética con distorsión EPI y caída de señal en RM de difusión/ADC (base del cráneo).

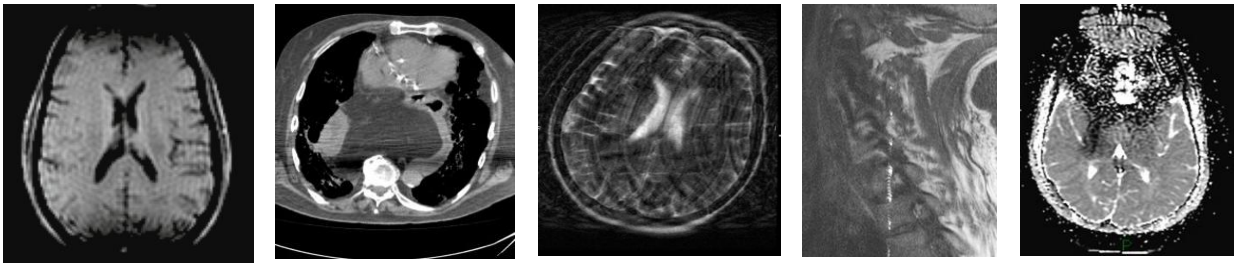

a) b) c) d) e)

## 2. MATERIALS AND METHODS

We conducted a scoping review following PRISMA-ScR guidance to map methods for MRI artifact correction across traditional/hybrid and deep learning approaches. Searches were run in Scopus and PubMed over the last five years and were complemented with hand-searching. We prioritized Scopus and PubMed due to their broad, curated coverage in engineering and medical sciences, complemented by targeted hand-searching of core venues. The choice of Scopus and PubMed reflects their editorial robustness (indexed journals, peer-reviewed proceedings) and continuous updates. Screening followed prespecified inclusion/exclusion criteria. We charted study attributes and grouped evidence by artifact type and approach (DL vs. traditional). The core synthesis comprises 18 primary studies (11 MRI+DL, 5 traditional/hybrid MRI). Two non-MRI papers (LSFM, CCTA) are reported only as contextual background, outside the core synthesis.

Based on the above, the search Equation (1) is proposed to extract the maximum number of scientific articles relevant to the objective of the review:

*("magnetic resonance imaging" OR MRI) AND (artifact* OR artefact*) AND (correct* OR reduc* OR mitigat* OR remov* OR suppress* OR compensat*) AND (method* OR technique* OR algorithm*)* (1)

Time window: 2020 – 2025.

Titles/abstracts were screened against inclusion/exclusion criteria, followed by full-text assessment. Two reviewers screened independently; disagreements were resolved by discussion. Data were charted using predefined fields: artifact type, MRI sequence and field strength, data (real vs. simulated), method family, metrics, code/data availability.

### *2.1. Inclusion criteria*

The inclusion criteria will enable the selection of articles that contribute to achieving the objective of this review. These criteria are outlined below:

- Primary studies on artifact correction in MRI (acquisition, reconstruction or post-processing).
- English, peer-reviewed journal or conference papers.
- Report methods, data (real/simulated), and metrics.
- Optional context-only: studies in related modalities strictly for translational context and excluded from core synthesis

### *2.2. Exclusion criteria*

The exclusion criteria will be used to remove articles that are not related to the objective of the review. The exclusion criteria are presented below:

- Non-MRI primary studies (excluded from core; may appear as context-only).
- Book chapters, theses, non-peer-reviewed items.
- Non-English.
- Outside the specified time window.
- Studies not addressing artifact correction

Due to the lack of articles on this specific problem, some papers are manually added that are directly related to the topic but may be in other official databases. Furthermore, consistent filters (date range, document type, subject area) were applied across both platforms to ensure traceability and comparability. The Scopus–PubMed combination showed high useful overlap with a low false-positive rate, streamlining full-text screening—unlike non-domain-specific bibliographic databases that added noise with minimal incremental yield.

## 3. RESULTS

In this section, the results of the methodology and the review will be presented, and the most important findings will be described.

### *3.1. Methodology*

Using the search equation and eligibility criteria, we identified records from Scopus and PubMed and removed duplicates (n=4). After title/abstract screening, 138 records were excluded. Ten articles underwent full-text assessment, of which 5 were excluded. Five additional records were found via hand-searching. In total, 18 records were included in the evidence base. The core synthesis comprises 18 primary studies, specifically 11 MRI+DL and 5 traditional/hybrid MRI; 2 non-MRI studies (LSFM, CCTA) are presented as context-only and are not counted in the core. See PRISMA-ScR flow in Figure 2.

Figure 2. Results of the PRISMA-ScR methodology for the artifacts review in MRI.

Figura 2. Resultados de la metodología PRISMA-ScR para la revisión de artefactos en IRM.

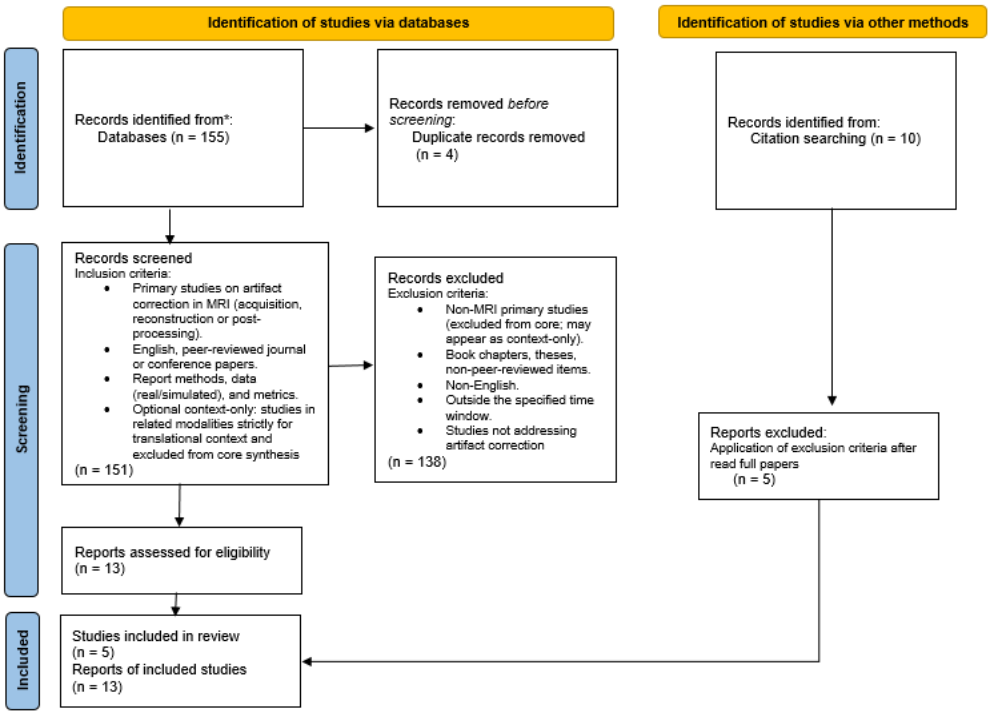


### *3.2. Review findings*

This section presents the findings of the review, which will help identify techniques, methods, and models used for correcting artifacts in magnetic resonance imaging.

#### 3.2.1. Types of MRI artifacts (causes and mitigation)

There are different types of MRI artifacts, such as motion, banding, Gibbs ringing, increased noise due to low SNR, fold-over/aliasing, among others. These artifacts may arise from acquisition setup, k-space processing, or physiological motion [2], [9-24].

To address some of these problems, physical improvements can be implemented to help prevent such artifacts [24]. However, some artifacts, such as motion artifacts, are particularly recurrent, as any patient movement can introduce noise into the image. In such cases, some authors suggest using breathing techniques or acquiring rapid images [2], [9-24].

On the other hand, many authors have applied statistical methods and Artificial Intelligence techniques to tackle this issue, either by reconstructing the image in k-space or by denoising the [2], [9-24]. Table 1 shows the types of artifacts, their causes and the most common way to mitigate them [24].

Table 1. Types of MRI artifacts, causes, and mitigation.

Tabla 1. Tipos de artefactos de resonancia magnética, causas y mitigación.

| Artifact | Type of artifact | Causes | Mitigation | Ref |
|---|---|---|---|---|
| **Motion artifacts** | Spin-echo sequence | Pulse sequence | An echo train with successive 90° pulses is employed to mitigate motion. | [2,25] |
| **Dark band artifacts** | bSSFP sequence | bSSFP sequence | Frequency scouts are utilized to detect off-resonance signals, TRs are kept short, and lower magnetic field strengths | [2] |
| **Increased noise due to low SNR** | GRE sequence | GREE sequence | Decreasing the signal bandwidth | [2] |
| **Fold-over artifacts** | Cartesian k-space sampling | Cartesian k-space sampling | Increasing the field of view (fov) or swapping the phase- and frequency-encoding directions | [2] |
| **B0-inhomogeneity artifacts or ecg synchronization errors** | Radial k-space sampling | Radial k-space sampling | Reducing the acceleration factor, employing frequency scouts to locate off-resonance, and incorporating self-navigation methods | [2] |
| **Main magnetic field b0-inhomogeneity** | Magnetic field inhomogeneity artifacts | Non-uniformity of the main magnetic field | Selective volumetric shimming and increasing spatial resolution | [15] |
| **Dielectric artifacts** | | B1 field inhomogeneity by another electric field | Dielectric pads or advanced coil designs | [16] |
| **Zipper artifacts** | Technical and hardware-related artifacts | Spurious RF contamination | Ensuring the scanner room door is closed, verifying the RF coil connection, and eliminating external rf sources in the mri room | [17] |
| **Zebra artifacts** | Technical and hardware-related artifacts | Interference with k-space data acquisition | Widening the field of view or using spin-echo-based sequences | [17] |
| **Magnetic susceptibility/metallic artifacts** | Magnetic field inhomogeneity artifacts | Prosthesis, surgical clips, screws, cardiac implantable electronic devices | Decreasing the voxel size or echo time, increasing the bandwidth, and employing gre sequences | [17,26] |
| **Chemical shift artifacts** | Sequence-specific and tissue heterogeneity artifacts | Misregistration of fat and water molecules | Changing the frequency-encoding direction, reducing the voxel size, or increasing the bandwidth | [18] |

| | | | | |
|---|---|---|---|---|
| **Off-resonance/dark band artifacts** | Magnetic field inhomogeneity artifacts | Magnetic field inhomogeneity at higher field strengths using bssfp sequence | Minimizing tr, applying higher-order shimming, and/or using a frequency scout map | [18,19] |
| **Aliasing/wrap-around artifacts** | Magnetic field inhomogeneity artifacts | Small fov | Increasing the fov, using saturation bands to suppress interfering signals | [20] |
| **Lge improper ti** | Sequence-specific and tissue heterogeneity artifacts | Inappropriate selection of ti in lge scout | Psir imaging or artificial intelligence techniques are employed to determine the appropriate ti | [21] |
| **Motion artifacts** | Patient artifacts<br><br>Transient artifacts in arterial phase | Cardiac motion from the beating heart, blood flow, respiratory motion and involuntary or voluntary body movement | - Hold respiration, parallel imaging, single-shot or real time techniques<br>- Short acquisition windows, compressed sensing, variable density k-t, low-rank, simultaneous multiparametric acquisition and reconstruction techniques<br>- Ai can be used for noise reduction, resolution enhancement, artifact removal, and recovery of undersampled data. | [9-15], [23], [24], [28-30] |
| **Aliasing artifacts** | | Cardiac and respiratory motion | - Radial trajectories, propeller and spiral sampling<br>- Parallel imaging<br>- Random undersampling with model-based sparsity<br>- Low rank<br>- Reconstructions or more recently relying on deep<br>- Learning based methods | [31-34] |
| **Stripe artifacts** | Scanner geometry<br><br>Subject issues | Problems with scanner or motion patient | Deep learning correction | [13,14] |

Figure 3 summarizes the MRI artifact landscape and maps each artifact family to the corresponding mitigation strategies.

3.2.2. MRI datasets used in the reviewed studies

Different datasets have been used for reconstruction or correction of medical images such as FastMRI (300 images 2D slices) [12,34]; dMRI (20 datasets, 300 volumes per each dataset) [13], CCTA (313 patients) [35], MRI (10 images) [6], LSFM (5860 images) [14], MRI (19 patients) [36], MRI (125 images) [11], MRI (975 images) [28], MRI (2013 images) [27], Cine CMRI (4000 patients, 10-12 image slices per each patient) [37,38]; Cine CMRI (512 cardiac MRI image slices) [8,39]; Cine CMRI (5 patients, 5 image slices per each patient) [8,40]; and Cine CMRI [30].

Most datasets are private or created by the authors, as this information is sensitive in nature, therefore it needs licenses of use or create your own dataset. Additionally, due to the complexity of acquisition and the size of the images, datasets tend to be small. It is complex to have a dataset with artifacts, some authors have created synthetics artifacts in their dataset [11,12,37].

The following MRI datasets were used in the included studies. In Table 2, we list one dataset per row and report size as stated by the original sources. Two additional non-MRI datasets—LSFM [14] and CCTA [35]—were identified; they are excluded from Table 2 as outside the MRI scope but are referenced for methodological relevance. It can be noted that a wide variety of approaches in image acquisition and the disparity in the size of each dataset. This feature allows to understand both the limitations and the generalization potential of the artifact correction methods, as each modality presents specific characteristics and challenges in the context of image reconstruction and improvement.

Figure 3. MRI artifact landscape and mitigation flow map.

Figura 3. Mapa de flujo de mitigación y panorama de artefactos de resonancia magnética.

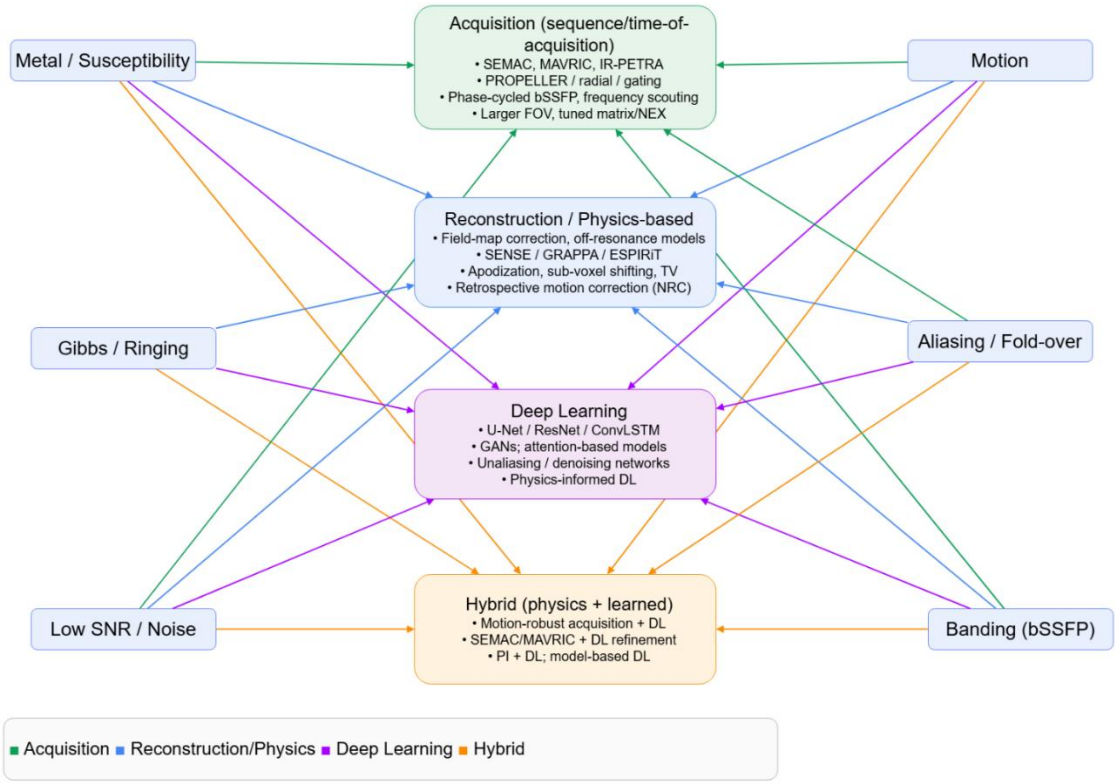


Table 2. Summary of reported datasets, their modalities, and their sizes.

Tabla 2. Resumen de los conjuntos de datos reportados, su modalidad y sus tamaños.

| Dataset | Imaging modality | Size | Reference |
|---|---|---|---|
| NYU fastMRI (knee) | Knee MRI (DICOM + k-space) | >10,000 clinical DICOM knee studies and >1,500 fully-sampled knee MRIs (k-space). | [12] |
| Own dataset | Neonatal dMRI | ~300 volumes per subject (typical dHCP-style protocol). | [13] |

| | | | |
|---|---|---|---|
| Own dataset | Brain MRI (low-field, if applicable) | n = 10 scans used in the study. | [6] |
| Own dataset | Brain MRI | 19 patients. | [36] |
| Own dataset | Brain MRI | 125 images. | [11] |
| UK Biobank (CMR) | Cine cardiac MRI | Program has >48,000 participants imaged; typical 6–12 short-axis slices per subject. | [37,38] |
| ACDC (Automated Cardiac Diagnosis Challenge) | Cine cardiac MRI | 150 patients (100 train, 50 test); 6–21 short-axis slices per exam. | [8,39] |
| Cedars-Sinai (prospective) | Cine cardiac MRI | 9 studies, 80 slices total; 8–13 slices per study; 70 for test and 10 for fine-tuning. | [8,40] |
| Own dataset | Cine cardiac MRI | 65 patients. | [30] |
| ADNI | Structural brain MRI | Large multi-site repository; order of tens of thousands of MRI images. | [28] |
| OASIS-3 | Structural brain MRI | ~1,098 participants and >2,000 MRI sessions (varies by release). | [27,41–44] |

### 3.2.3. Deep Learning-based methods for correction of artifacts

Recent advances in deep learning have strengthened artifact correction capabilities, showing its usefulness in mitigating the effects of issues such as patient motion, undersampling artifacts, and slice-to-slice inconsistencies. This has allowed us to improve the quality of diagnostic images, optimize acquisition times and precision in clinical environments.

An area of interest in the literature is how deep learning-based methods handle motion-induced artifacts, a common challenge that affects the reliability and consistency of images in clinical and research applications [27]. Furthermore, advanced artifact removal techniques, such as methods based on residual neural networks with attention mechanisms, have shown great potential to address similar problems in other biomedical imaging modalities, such as light sheet fluorescence microscopy (LSFM) [14], techniques that can be extended to MRI.

Below are the main approaches organized by the types of artifacts they address:

*Motion artifact correction:*

A transformer-based architecture presented by [30] uses attention mechanisms to combine local and global contextual features, achieving accurate motion estimates even in highly accelerated studies. In [10] A convolutional neural network (CNN)-based method for dynamic contrast-enhanced MRI is introduced, which combines multi-scale feature extraction and attention mechanisms, achieving a PSNR of 35.212 dB and an SSIM of 0.974. In [27] uses deep learning-based segmentation methods such as FastSurferCNN, Kwyk, and ReSeg, which demonstrated greater consistency in brain segmentation in images affected by motion artifacts compared to traditional tools such as FreeSurfer. On cardiac MRI [8], A recurrent neural network was developed with bidirectional ConvLSTM branches, allowing effective extraction of spatio-temporal features and improving image quality in the presence of motion.

*Reduction of undersampling artifacts:*

In [36] a spatio-temporal approach for radial cardiac MRI is proposed, using a modified U-Net that outperforms existing 2D and 3D techniques in image quality and reconstruction times. For low-field MR

images, a residual U-Net combined with data augmentation is presented, which preserves global structure and fine details even with limited training data [6].

*Inconsistencies between slices:*

The dStripe method, introduced by [13], corrects intensity variations between slices in diffusion MRI using a multiplicative field-based approach, improving image quality without introducing bias.

*Removal of stripe artifacts:*

In [14] presents a method based on residual neural networks with attention modules (Att-ResNet) to remove streak artifacts in light sheet fluorescence microscopy (LSFM) images. This approach uses an enhanced U-Net encoder-decoder structure with residual blocks and attention, achieving improvements in PSNR and SSIM compared to classical and other deep learning-based methods. Although developed for LSFM, this method has the possibility of being adapted to magnetic resonance imaging and other modalities affected by stripe artifacts or similar.

*Integrated artifact correction:*

In [37] proposes an approach for the detection, correction and segmentation of artifacts in cardiac MR images, transforming the problem into an optimized reconstruction task with a joint loss function. In [9] presents MARC, a CNN-based artifact reduction method for dynamic liver MRI. This approach improves image quality without requiring additional scanning time, although it faces generalization challenges between different sequences.

*Specific applications:*

In breast diagnosis, [35] develops a decision support system for lesions using a two-stage segmentation approach, integrating deep learning and traditional techniques for breast cancer detection.

Although advances in deep learning are significant, limitations remain. Among others, the most significant are:

- Many studies rely on small data sets, which can restrict generalizability ([11,36]).
- Some methods tend to over-smooth motion estimates in images with severe artifacts [6,30].
- Integration of 3D volumetric techniques and multimodal approaches remains a major challenge [30,42].
- Difficulties in generalization in cases that are outside the standard training conditions [27].
- Reliance on high-quality training data to achieve effective stripe artifact removal, which could limit its applicability in clinical settings with complex noise or insufficient data [14].

Despite the limitations of the area, the integration of attention mechanisms, spatio-temporal analysis and architectures such as those used in [8,14,37], show progress in correcting MRI artifacts. Additionally, the literature shows that deep learning-based methods are not only faster, but also more consistent under challenging conditions [27], which reinforces its clinical potential. On the other hand, the approach Att-ResNet [14] opens new possibilities for stripe artifact removal and could be adapted to MR modalities affected by similar problems. Future studies in this area should focus on expanding data sets, improving model generalization, and exploring hybrid approaches that combine the best of traditional and deep learning-based methods.

Table 3. presents a summary of Deep Learning-based methods for artifact correction, detailing the architecture, loss function, and metrics used.

Tabla 3. Presenta un resumen de los métodos basados en Deep Learning para la corrección de artefactos, detallando la arquitectura, función de pérdida y métricas usadas.

| **Method** | **Artifact/ Medical Image** | **Architecture** | **Loss** | **Metrics** | **Hyperparameters** | **Library/ Framework** |
|---|---|---|---|---|---|---|
| Deep Learning reconstruction [30] | Aliasing/ CMRI | Vit-V-Net and TransMorph | Photometric<br>MSE<br>Smoothness<br>NRMSE<br>HFEN | SSIM 0.85±0.05<br>PSNR 40.97±3.65<br>NRMSE 0.18±0.08<br>HFEN 1.87±+0.77<br>Lphoto 5.36±2.86 | Optimizer: AdamW<br>LR Scheduler: $5x10^{-4}$ | Pytorch |
| Deep Learning motion reduction [8] | Aliasing/ CMRI | Recurrent GAN bi-directional ConvLSTM | Wasserstein distance and gradient penalty for discriminator<br>Perceptual loss for generator | SSIM 0.884±0.047<br>PSNR 28.514±2.210 | Optimizer: Adam<br>LR: $10^{-4}$<br>Epochs: 50<br>Mini-batches: 4 | Pytorch |
| Deep Learning correction [37] | Motion/ CMRI | A k-space line detection network<br>RCNN for correction<br>U-Net for image segmentation | Cross-entropy<br>MSE<br>Pixel-wise cross entropy | MAE: 0.048<br>PSNR: 28.805<br>SSIM: 0.801<br>SI: 75.819 | Optimizer: Adam<br>Momentum: 0.9<br>LR: $5x10^{-4}$<br>Activation: ReLU | Pytorch |
| Deep Learning correction [9] | Motion/ MRI | CNN | L1 Loss | SSIM: 0.91±0.07 | Optimizer: Adam<br>LR: $10^{-3}$<br>Epochs: 100<br>Batch size: 64<br>Activation: ReLU | Keras |
| Deep Learning correction [10] | Motion/ MRI | U-NET/CNN/ AttentionBlock | MS-SSIM Loss | PSNR: 35.21±3.321<br>SSIM: 0.974±0.015 | Optimizer: Adam<br>LR: $10^{-3}$<br>Epochs: 30<br>Activation: ReLU | Pytorch |
| Deep Learning correction [11] | Motion/ MRI | DRN-DCMB | MSE | SSIM: 0.957±0.025<br>ISNR: 4.44±1.45 | Optimizer: Adam<br>LR: $10^{-3}$<br>Epochs: 50<br>Mini batches: 50<br>Activation: ReLU | Tensorflow |
| Deep Learning correction [36] | Unknown/ MRI | U-NET/CNN | L2 Error | PSNR: 40.376<br>SSIM: 0.954<br>HPSI: 0.989<br>NRMSE: 0.079 | Optimizer: SGD<br>LR: $10^{-5}$<br>Activation: ReLU | |
| Deep Learning correction-reconstruction [13] | Stripe/ dMRI | CNN | MC SURE | DTI<br>MT CSD | Optimizer: Adam<br>Epochs: 500<br>Triangular LRS<br>Activation: ReLU | Pytorch |

| | | | | | | |
|---|---|---|---|---|---|---|
| Deep Learning correction [6] | Unknown/ MRI | U-NET | MSE | PSNR: 26.52±2.22<br>SSIM 0.80±0.02<br>NRMSE: 0.07±0.03 | Optimizer: RMSProp<br>LR: $3x10^{-3}$<br>Epochs: 2000<br>Activation: ReLU | Tensorflow/ Keras |
| Deep Learning correction [12] | Motion/ MRI | kLDNet based in U-NET | L1-SSIM Loss | SSIM: 0.99±1.82<br>PSNR: 44.82±6.44<br>HPSI: 97.33±5.56<br>Accuracy: 97.06 | Optimizer: Adam<br>LR: $10^{-4}$<br>Epochs: 4200<br>Batch Size: 4<br>Activation: ReLU | Pytorch |
| AIR Recon DL by GE Healthcare (enhance quality) [45] | MRI | CNN | | | | |
| Deep learning correction [27] | MRI | ReSeg<br>FastSurferCNN | Focal Loss<br>Generalised Dice Loss | DSC<br>HD | Optimizer: RMSProp<br>LR: $10^{-4}$<br>Batch Size: 8 vols.<br>Epochs: Early Stopping - 20 patient | Tensorflow |

For completeness, we note two non-MRI deep-learning entries that are excluded from Table 3 to keep it MRI-specific but remain cited for methodological affinity. LSFM [14] addresses stripe artifacts with a U-Net + CBAM model trained in TensorFlow/Keras using MAE and content loss (Adam; ~300 epochs, batch size 2), reporting MAE 6.06 ± 1.50, PSNR 30.56 ± 1.85, and SSIM 0.92 ± 0.05. CCTA [35] targets motion with a Pix2Pix/U-Net pipeline (MATLAB), reporting PSNR 26.1, SSIM 0.86, DSC 0.783, and HD 4.47. These non-MRI results are referenced only in the text and are not counted in the core synthesis.

3.2.4. Other type of methods for correction of artifacts

Other methods for mitigating artifacts in medical images can be classified into two groups: hardware (focused on physically modifying the acquisition environment) and software (programs for image correction) (see Table 4).

Below are some approaches organized by the types of artifacts they address:

*Hardware Related Spatial Distortions (HRSD):*

These distortions vary depending on the scanner configuration and the intensity of the magnetic field, directly affecting the spatial precision of the images. The IR-PETRA (Inversion Recovery Point Encoding Time Reduction with Radial Acquisition) sequence exhibits variable levels of HRSD. On 3.0 T scanners, adequate spatial precision was achieved without the need for correction algorithms. On 1.5 T scanners, distortion correction techniques were required to achieve comparable levels of accuracy [25]. In this scenario, adjusting acquisition strategies based on hardware minimizes distortions.

*Motion-related artifact:*

Patient movement remains a major source of artifacts. In this sub-category of work, various strategies have been developed to mitigate its impact:

- *Dynamic abdominal MRI with contrast:* A study in 325 patients demonstrated that image quality directly correlates with the degree of abdominal movement, evaluated by respiratory wave analysis. Images without abdominal movement showed no artifacts, highlighting the importance of controlling patient movement [28].

- *Cranial magnetic resonance imaging:* The use of the PROPELLER (*Periodically Rotated Overlapping Parallel Lines with Enhanced Reconstruction*) technique has been reported. This approach combines redundant data from multiple acquisition angles to reduce motion artifacts. In [32], Using a "pause" function during acquisition was shown to significantly improve image quality by repositioning the object, achieving increases in SSIM from 0.52 to 0.80.

- *Non-rigid motion correction (NRC):* In the field of cardiac resonance, NRC has been shown to be superior to translational techniques, improving image quality and contrasts between cardiac tissues under free breathing conditions. Furthermore, it allowed a more precise quantification of late enhancement masses, which could significantly benefit the diagnosis of cardiac pathologies. [29].

*Impact of metallic implants on image quality:*

Artifacts generated by metallic implants, such as those made of titanium or cobalt-to-chromium, are still a challenge. Various studies have evaluated how to mitigate these effects:

- Polarization of the B1 field: In hip MRI [26], was shown that at 1.5 T, circular polarization was effective in reducing the size of acetabular cup artifacts and femoral necrolysis. At 3.0 T, elliptical polarization outperformed 1.5 T techniques in the femoral stem region, achieving significant reductions in artifacts.

- Advanced techniques such as HBW-TSE and SEMAC: These methodologies have improved the correction of metallic artifacts, highlighting the complex interactions between magnetic field strength, RF pulse polarization, and implant material. This could indicate that different MRI techniques should be considered depending on the type of implant and the anatomical region of interest [26].

Despite advances in traditional techniques, several important challenges remain. Hardware-related distortions depend significantly on scanner settings, requiring custom adjustments to ensure adequate accuracy. Patient movement artifacts are difficult to predict in pediatric populations or critically ill patients, where movement control is limited. In the case of metallic implants, the effectiveness of current techniques is influenced by the type of implant and the anatomical region, which limits their general applicability.

Although techniques such as NRC and PROPELLER have improved image quality, their effectiveness still needs additional validation in larger populations to ensure robustness and generalizability.

Directions for future work in this field should be considered: validation of these techniques in broader populations with greater diversity of clinical conditions. The integration of hybrid approaches that combine traditional and advanced strategies, such as deep learning, to optimize artifact correction. Exploring automated methods to customize hardware configurations and acquisition parameters to patient needs.

Table 4. Artifact correction methods based on their type (hardware or software).

Tabla 4. Métodos de corrección de artefactos basado en su tipo (hardware o software).

| Medical Image | Method | Type of method |
|---|---|---|
| MRI | IR-PETRA [25] | Hardware |
| MRI | SEMAC [26] | Hardware |
| MRI | PROPELLER [32] | Software |
| CMRI | NRC (non-rigid motion correction) [29] | Software |

## 4. DISCUSSION

### 4.1 General aspects

Leveraging Scopus and PubMed ensured editorial quality and domain-wide coverage while minimizing dispersion across less pertinent databases—unlike non-domain-specific sources that tended to increase noise with minimal incremental yield.

Artifact removal in magnetic resonance imaging (MRI) requires the integration of diverse efforts. From acquisition-time strategies (e.g., SEMAC, IR-PETRA, PROPELLER) to reconstruction/post-processing approaches (e.g., iterative SENSE), each strategy responds to specific clinical challenges, such as the presence of metallic implants or the control of motion artifacts. However, in clinical practice, the availability of resources and the heterogeneity of acquisition protocols require a constant search for adaptable methods that offer good results in different circumstances. As a response to this, the community has explored the incorporation of deep learning solutions, often artifact-specific, with some early attempts at multi-artifact correction, but also pose their own challenges such as the costs associated with computing for training large models, as well as the availability of data in sufficient quantities to infer patterns that allow generalization. These observations reflect the core synthesis of primary studies, with two non-MRI papers cited only as contextual background.

From the review, we identified a typical approach sequence (Figure 4): MRI data are started, which, after preprocessing and labeling, are then transferred to post-acquisition correction methods—both reconstruction/physics and deep learning and hybrid approaches. A stepwise evaluation combining image quality metrics with task- and reader-study-level metrics is then applied. Generalization across sequences, fields, and centers is then verified, along with safeguards and reporting; all of this converges in clinical preparation.

Figure 4. Typical evaluation and reporting workflow for MRI artifact correction.

Figura 4. Secuencia típica de evaluación y reporte en la corrección de artefactos en MRI.

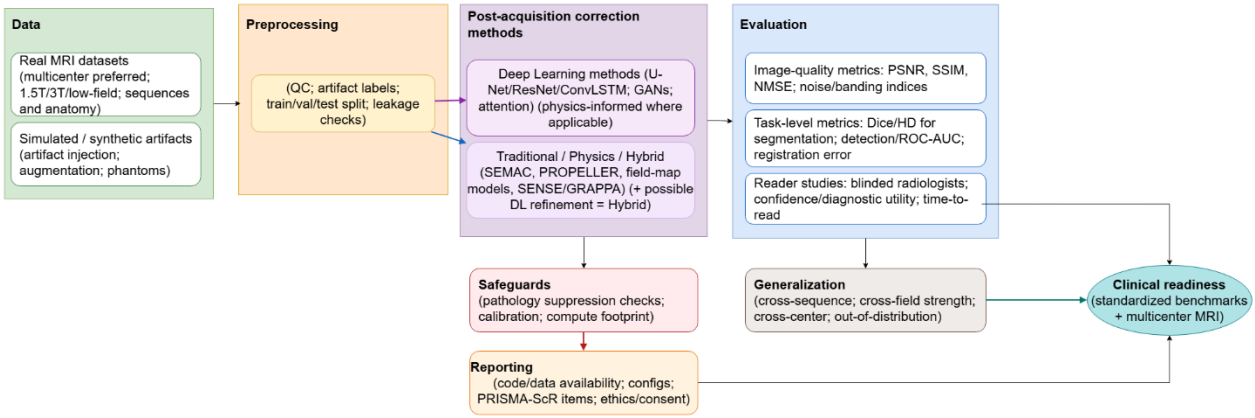


Traditional techniques, both hardware and software, usually offer great robustness in specific scenarios. Methods such as SEMAC minimize metal-induced distortion, while PROPELLER effectively mitigates motion artifacts in brain sequences. However, these systems do not usually cover all the artifacts that may arise (aliasing, stripes).

On the other hand, deep learning-based methods stand out for their ability to process large volumes of data and learn complex noise or distortion patterns. In recent studies, they have achieved significant increases in

metrics such as PSNR and SSIM, demonstrating high effectiveness against motion artifacts and aliasing. However, they still face limitations related to the need for large quality databases and the difficulty of generalizing to different populations and acquisition parameters.

Some of the challenges that remain:

- Scarcity and variability of datasets: many studies use small image sets or simulate artifacts, which can limit the external validity of the results and the ability of the models to deal with exceptional clinical cases.
- Multicenter clinical validation: most of the advances have been evaluated in controlled environments; Collaborative studies involving hospitals with different MRI equipment and protocols are lacking.
- Computational cost and technical expertise: Training deep neural networks requires specialized hardware and trained personnel, aspects that may not be available in all health centers.
- Standardization and integration: The existence of various acquisition methods and parameters makes it difficult to adopt a standard for artifact correction. Therefore, hybrid approaches are sought that combine the robustness of traditional techniques with the adaptability of machine learning techniques.

4.2 The use of deep learning methods

In this context, architectures ranging from conventional convolutional neural networks (CNN) to attention-based approaches (transformers), including U-Net and GAN, have been studied. In general, U-Net and its variants have shown high versatility for the correction of local artifacts such as streaks or aliasing, while attention-based models seem more promising when capturing broader correlations, typical of extensive motion deformations, is required.

Regarding quality metrics, PSNR and SSIM are the image quality metrics that predominate in the literature, measuring residual noise intensity and structural similarity, respectively. Across the included MRI studies, SSIM ≈ 0.95–0.97 and PSNR ≈ 35–45 dB are commonly reported under study-specific settings, indicating notable improvements in final quality. Even so, the comparison of results between studies can be affected by the use of different acquisition protocols, anatomical regions, and training configurations.

Regarding cost functions and optimization methods, they commonly use functions such as MSE, MAE or MS-SSIM. The Adam optimizer and its variants stand out for their stability in the search for minimums. It is evident that given the availability of data, it is necessary to focus on the adjustment of hyperparameters such as batch size, learning rate, number of epochs. When the training set was scarce, the literature showed that they could resort to the generation of synthetic artifacts or data augmentation techniques, in order to strengthen the generalization capacity.

In this particular context, limitations still persist:

- *Dependence on large volumes of data:* the lack of extensive and heterogeneous databases remains a problem, especially in applications where artifacts have low clinical prevalence or there are high privacy requirements.

- *Possible suppression of pathological signals:* A critical aspect of artifact correction using neural networks is the possibility that noise or artifact removal may inadvertently suppress some of the relevant pathological signals. For example, low-contrast lesions or subtle alterations in signal intensity could be altered or smoothed, negatively impacting the diagnosis. In this context, it is important to have comprehensive clinical validations and evaluation methods that involve both image quality metrics (PSNR, SSIM) and qualitative assessments by experts.

- *Computational requirements:* the complexity of deep neural networks increases the cost of training and inference, which makes mass adoption difficult in centers with limited resources. The availability and access to technological infrastructure is increasing, however, thinking about the construction of large foundational models for artifact correction maximizes the limitations in this aspect.

- *Generalization to different sequences and magnets:* models trained with a specific type of sequence and magnetic field may not work optimally in different contexts, they are very limited to biotype patterns, technology and specific protocols. Therefore, it is still characteristic to find works that try to correct artifacts in very particular conditions and domains.

- *Correlation with improvements in real clinical practice:* It is common in the literature to report significant improvements in image quality metrics such as PSNR and SSIM. However, further studies are still needed to establish the correlation between improvements in the metrics and improvements in real clinical practice. The extent to which a more artifact-free image impacts a more accurate diagnosis and, ultimately, favorable clinical outcomes must be evaluated. Several authors have suggested that, in addition to quantitative metrics, it is essential to include reading studies or validations with experienced radiologists to determine whether artifact suppression positively influences the identification of lesions and the establishment of therapeutic measures.

The field of deep learning is one of the most active fields of science. The research and development of new models is dizzying, in this scenario the possible trends will depend on these same dynamics in the sense that new mathematical theories or architectures could limit the initiatives to develop models with current architectures. However, we can establish in general terms:

- Hybrid models: Combining traditional techniques (SEMAC, PROPELLER) with neural network architectures could allow for more robust corrections that are less dependent on extensive data.

- Creating large repositories: advancing initiatives that bring together images from multiple centers with different protocols and populations, ensuring anonymization and compliance with ethical aspects, in massive quantities, will allow the idea of building large foundational models for artifact correction, or at least moving in the direction of generalization between modalities.

- Improved explainability: Interpretability methods aimed at helping radiologists understand the transformation that the network performs on the image, reducing diagnostic uncertainty, are desirable in this field as in any other AI application domain. However, the community has not yet developed general extensible methods between architectures. It seems that a trade-off must be made between the benefits of these techniques and the loss of explainability of their results.

- Integration of attention architectures: The incorporation of mechanisms that optimize self-attention, such as efficient attention mechanisms (e.g., windowed or linear attention), is emerging as a promising way to capture global correlations in the image and correct artifacts in dynamic or long sequences.

4.3 Ethical considerations

Although the studies analyzed report the use of anonymized data to train deep learning models, the ethical and legal implications remain an aspect to consider. As a scoping review, we did not access individual-level data; we summarized how primary studies reported consent/approval and de-identification. Privacy regulations, such as those in Europe [46] and the United States [47], require strengthening data protection and transparency in its use. This aspect must be considered so that the anonymization process does not affect the quality and representativeness of the data in the construction of unbiased models that generalize appropriately.

In this work, we recognize these ethical implications; however, since the focus was on the review of artifact correction methods, the legal dimension was not explored in depth.

4.4 Study limitations

An important limitation of this study is the small number of articles finally included. This aspect is explained, in large part, by the nature of most works related to artifacts from the physical perspective of the acquisition process, however, our focus was on the correction of artifacts once they were generated. The five-year window and the use of Scopus/PubMed (plus hand-searching) may have missed earlier or non-indexed works. Although other databases were not included, the robustness of Scopus and PubMed, complemented by targeted hand-searching, mitigated the risk of missing relevant studies. As a scoping synthesis, we did not perform a quantitative meta-analysis or a formal risk-of-bias assessment; heterogeneity in datasets, sequences, and metrics precluded pooling.

## 5. CONCLUSIONS

Artifact correction in MRI benefits from both traditional approaches, such as hardware-oriented solutions and software techniques, and DL methods show strong gains for specific artifact types and settings; broader multi-artifact generalization remains an open goal. However, deep learning approaches critically rely on large-scale, high-quality data sets and specialized computational resources, while traditional solutions, although more specific, show robust performance in well-defined scenarios.

Recent studies indicate that hybrid strategies, combining physical adjustments with deep neural networks, improve artifact mitigation while generally preserving diagnostic details. Still, limitations remain, including the risk of removing or altering true pathological signals due to artifact-removal modifications, highlighting the need for explainable models and rigorous clinical validation. Data sharing practices must also improve to ensure diverse training sets and broader applicability of these techniques. Ultimately, the integration of traditional and AI-based solutions, along with consistent multi-center assessments and transparent correction processes, appears to be the most promising avenue for advancing MRI imaging quality and diagnostic accuracy.

## References

1. Gallo-Bernal, S.; Bedoya, M.A.; Gee, M.S.; Jaimes, C. Pediatric Magnetic Resonance Imaging: Faster Is Better. *Pediatr Radiol* **2023**, *53*, 1270–1284, doi:10.1007/s00247-022-05529-x.

2. Ferreira, P.F.; Gatehouse, P.D.; Mohiaddin, R.H.; Firmin, D.N. Cardiovascular Magnetic Resonance Artefacts. *Journal of Cardiovascular Magnetic Resonance* **2013**, *15*, 41, doi:10.1186/1532-429X-15-41.
3. Ensle, F.; Kaniewska, M.; Tiessen, A.; Lohezic, M.; Getzmann, J.M.; Guggenberger, R. Diagnostic Performance of Deep Learning-Based Reconstruction Algorithm in 3D MR Neurography. *Skeletal Radiol* **2023**, *52*, 2409–2418, doi:10.1007/s00256-023-04362-z.
4. Filli, L.; Jungmann, P.M.; Zingg, P.O.; Rüdiger, H.A.; Galley, J.; Sutter, R.; Pfirrmann, C.W.A. MRI with State-of-the-Art Metal Artifact Reduction after Total Hip Arthroplasty: Periprosthetic Findings in Asymptomatic and Symptomatic Patients. *Eur Radiol* **2020**, *30*, 2241–2252, doi:10.1007/s00330-019-06554-5.
5. Boutet, A.; Madhavan, R.; Elias, G.J.B.; Joel, S.E.; Gramer, R.; Ranjan, M.; Paramanandam, V.; Xu, D.; Germann, J.; Loh, A.; et al. Predicting Optimal Deep Brain Stimulation Parameters for Parkinson's Disease Using Functional MRI and Machine Learning. *Nat Commun* **2021**, *12*, 3043, doi:10.1038/s41467-021-23311-9.
6. Ayde, R.; Senft, T.; Salameh, N.; Sarracanie, M. Deep Learning for Fast Low-Field MRI Acquisitions. *Sci Rep* **2022**, *12*, 11394, doi:10.1038/s41598-022-14039-7.
7. Captur, G.; Bhandari, A.; Brühl, R.; Ittermann, B.; Keenan, K.E.; Yang, Y.; Eames, R.J.; Benedetti, G.; Torlasco, C.; Ricketts, L.; et al. T1 Mapping Performance and Measurement Repeatability: Results from the Multi-National T1 Mapping Standardization Phantom Program (T1MES). *J Cardiovasc Magn Reson* **2020**, *22*, 31, doi:10.1186/s12968-020-00613-3.
8. Lyu, Q.; Shan, H.; Xie, Y.; Kwan, A.C.; Otaki, Y.; Kuronuma, K.; Li, D.; Wang, G. Cine Cardiac MRI Motion Artifact Reduction Using a Recurrent Neural Network. *IEEE Transactions on Medical Imaging* **2021**, *40*, 2170–2181, doi:10.1109/TMI.2021.3073381.
9. Tamada, D.; Kromrey, M.-L.; Ichikawa, S.; Onishi, H.; Motosugi, U. Motion Artifact Reduction Using a Convolutional Neural Network for Dynamic Contrast Enhanced MR Imaging of the Liver. *Magn Reson Med Sci* **2020**, *19*, 64–76, doi:10.2463/mrms.mp.2018-0156.
10. Zhao, B.; Liu, Z.; Ding, S.; Liu, G.; Cao, C.; Wu, H. Motion Artifact Correction for MR Images Based on Convolutional Neural Network. *Optoelectron. Lett.* **2022**, *18*, 54–58, doi:10.1007/s11801-022-1084-z.
11. Liu, J.; Kocak, M.; Supanich, M.; Deng, J. Motion Artifacts Reduction in Brain MRI by Means of a Deep Residual Network with Densely Connected Multi-Resolution Blocks (DRN-DCMB). *Magnetic Resonance Imaging* **2020**, *71*, 69–79, doi:10.1016/j.mri.2020.05.002.
12. Al-Haj Hemidi, Z.; Weihsbach, C.; Heinrich, M.P. IM-MoCo: Self-Supervised MRI Motion Correction Using Motion-Guided Implicit Neural Representations. In Proceedings of the Medical Image Computing and Computer Assisted Intervention – MICCAI 2024; Linguraru, M.G., Dou, Q., Feragen, A., Giannarou, S., Glocker, B., Lekadir, K., Schnabel, J.A., Eds.; Springer Nature Switzerland: Cham, 2024; pp. 382–392.
13. Pietsch, M.; Christiaens, D.; Hajnal, J.V.; Tournier, J.-D. dStripe: Slice Artefact Correction in Diffusion MRI via Constrained Neural Network. *Med Image Anal* **2021**, *74*, 102255, doi:10.1016/j.media.2021.102255.
14. Wei, Z.; Wu, X.; Tong, W.; Zhang, S.; Yang, X.; Tian, J.; Hui, H. Elimination of Stripe Artifacts in Light Sheet Fluorescence Microscopy Using an Attention-Based Residual Neural Network. *Biomed Opt Express* **2022**, *13*, 1292–1311, doi:10.1364/BOE.448838.
15. Saremi, F.; Grizzard, J.D.; Kim, R.J. Optimizing Cardiac MR Imaging: Practical Remedies for Artifacts. *RadioGraphics* **2008**, *28*, 1161–1187, doi:10.1148/rg.284065718.
16. Alfudhili, K.; Masci, P.G.; Delacoste, J.; Ledoux, J.-B.; Berchier, G.; Dunet, V.; Qanadli, S.D.; Schwitter, J.; Beigelman-Aubry, C. Current Artefacts in Cardiac and Chest Magnetic Resonance Imaging: Tips and Tricks. *British Journal of Radiology* **2016**, *89*, 20150987, doi:10.1259/bjr.20150987.

17. Stadler, A.; Schima, W.; Ba-Ssalamah, A.; Kettenbach, J.; Eisenhuber, E. Artifacts in Body MR Imaging: Their Appearance and How to Eliminate Them. *Eur Radiol* **2007**, *17*, 1242–1255, doi:10.1007/s00330-006-0470-4.
18. Noda, C.; Ambale Venkatesh, B.; Wagner, J.D.; Kato, Y.; Ortman, J.M.; Lima, J.A.C. Primer on Commonly Occurring MRI Artifacts and How to Overcome Them. *RadioGraphics* **2022**, *42*, E102–E103, doi:10.1148/rg.210021.
19. Rajiah, P.; Bolen, M.A. Cardiovascular MR Imaging at 3 T: Opportunities, Challenges, and Solutions. *RadioGraphics* **2014**, *34*, 1612–1635, doi:10.1148/rg.346140048.
20. Zimmerman, S.L. Aliasing Artifact in Phase-Contrast Cardiac MR. In *Pearls and Pitfalls in Cardiovascular Imaging: Pseudolesions, Artifacts, and Other Difficult Diagnoses*; Fishman, E.K., Zimmerman, S.L., Eds.; Cambridge University Press: Cambridge, 2015; pp. 159–161 ISBN 978-1-107-02372-7.
21. Kellman, P.; Arai, A.E. Cardiac Imaging Techniques for Physicians: Late Enhancement. *J Magn Reson Imaging* **2012**, *36*, 529–542, doi:10.1002/jmri.23605.
22. van Heeswijk, R.B.; Bonanno, G.; Coppo, S.; Coristine, A.; Kober, T.; Stuber, M. Motion Compensation Strategies in Magnetic Resonance Imaging. *Crit Rev Biomed Eng* **2012**, *40*, 99–119, doi:10.1615/critrevbiomedeng.v40.i2.20.
23. Lin, D.J.; Johnson, P.M.; Knoll, F.; Lui, Y.W. Artificial Intelligence for MR Image Reconstruction: An Overview for Clinicians. *J Magn Reson Imaging* **2021**, *53*, 1015–1028, doi:10.1002/jmri.27078.
24. Rafiee, M.J.; Eyre, K.; Leo, M.; Benovoy, M.; Friedrich, M.G.; Chetrit, M. Comprehensive Review of Artifacts in Cardiac MRI and Their Mitigation. *Int J Cardiovasc Imaging* **2024**, *40*, 2021–2039, doi:10.1007/s10554-024-03234-4.
25. Ahmadian, S.; Jabbari, I.; Bagherimofidi, S.M.; Saligheh Rad, H. Characterization of Hardware-Related Spatial Distortions for IR-PETRA Pulse Sequence Using a Brain Specific Phantom. *Magn Reson Mater Phy* **2021**, *34*, 213–228, doi:10.1007/s10334-020-00863-3.
26. Khodarahmi, I.; Kirsch, J.; Chang, G.; Fritz, J. Metal Artifacts of Hip Arthroplasty Implants at 1.5-T and 3.0-T: A Closer Look into the B1 Effects. *Skeletal Radiol* **2021**, *50*, 1007–1015, doi:10.1007/s00256-020-03597-4.
27. Kemenczky, P.; Vakli, P.; Somogyi, E.; Homolya, I.; Hermann, P.; Gál, V.; Vidnyánszky, Z. Effect of Head Motion-Induced Artefacts on the Reliability of Deep Learning-Based Whole-Brain Segmentation. *Sci Rep* **2022**, *12*, 1618, doi:10.1038/s41598-022-05583-3.
28. Ikeno, H.; Kobayashi, S.; Kozaka, K.; Ogi, T.; Inoue, D.; Yoneda, N.; Yoshida, K.; Ohno, N.; Gabata, T.; Kitao, A. Relationship between the Degree of Abdominal Wall Movement and the Image Quality of Contrast-Enhanced MRI: Semi-Quantitative Study Especially Focused on the Occurrence of Transient Severe Motion Artifact. *Jpn J Radiol* **2020**, *38*, 165–177, doi:10.1007/s11604-019-00896-2.
29. Zeilinger, M.G.; Kunze, K.-P.; Munoz, C.; Neji, R.; Schmidt, M.; Croisille, P.; Heiss, R.; Wuest, W.; Uder, M.; Botnar, R.M.; et al. Non-Rigid Motion-Corrected Free-Breathing 3D Myocardial Dixon LGE Imaging in a Clinical Setting. *Eur Radiol* **2022**, *32*, 4340–4351, doi:10.1007/s00330-022-08560-6.
30. Ghoul, A.; Pan, J.; Lingg, A.; Kübler, J.; Krumm, P.; Hammernik, K.; Rueckert, D.; Gatidis, S.; Küstner, T. Attention-Aware Non-Rigid Image Registration for Accelerated MR Imaging. *IEEE Transactions on Medical Imaging* **2024**, *43*, 3013–3026, doi:10.1109/TMI.2024.3385024.
31. Kim, S.; Park, H.; Park, S.-H. A Review of Deep Learning-Based Reconstruction Methods for Accelerated MRI Using Spatiotemporal and Multi-Contrast Redundancies. *Biomed. Eng. Lett.* **2024**, *14*, 1221–1242, doi:10.1007/s13534-024-00425-9.
32. Saotome, K.; Matsumoto, K.; Kato, Y.; Ozaki, Y.; Nagai, M.; Hasegawa, T.; Tsuchiya, H.; Yamao, T. Improving Image Quality Using the Pause Function Combination to PROPELLER Sequence in Brain MRI: A Phantom Study. *Radiol Phys Technol* **2024**, *17*, 518–526, doi:10.1007/s12194-024-00784-z.

33. Zhang, L.; Jiang, B.; Chen, Q.; Wang, L.; Zhao, K.; Zhang, Y.; Vliegenthart, R.; Xie, X. Motion Artifact Removal in Coronary CT Angiography Based on Generative Adversarial Networks. *Eur Radiol* **2023**, *33*, 43–53, doi:10.1007/s00330-022-08971-5.
34. Knoll, F.; Zbontar, J.; Sriram, A.; Muckley, M.J.; Bruno, M.; Defazio, A.; Parente, M.; Geras, K.J.; Katsnelson, J.; Chandarana, H.; et al. fastMRI: A Publicly Available Raw k-Space and DICOM Dataset of Knee Images for Accelerated MR Image Reconstruction Using Machine Learning. *Radiology: Artificial Intelligence* **2020**, *2*, e190007, doi:10.1148/ryai.2020190007.
35. Zhang, L.; Jiang, B.; Chen, Q.; Wang, L.; Zhao, K.; Zhang, Y.; Vliegenthart, R.; Xie, X. Motion Artifact Removal in Coronary CT Angiography Based on Generative Adversarial Networks. *Eur Radiol* **2023**, *33*, 43–53, doi:10.1007/s00330-022-08971-5.
36. Kofler, A.; Dewey, M.; Schaeffter, T.; Wald, C.; Kolbitsch, C. Spatio-Temporal Deep Learning-Based Undersampling Artefact Reduction for 2D Radial Cine MRI With Limited Training Data. *IEEE Trans Med Imaging* **2020**, *39*, 703–717, doi:10.1109/TMI.2019.2930318.
37. Oksuz, I.; Clough, J.R.; Ruijsink, B.; Anton, E.P.; Bustin, A.; Cruz, G.; Prieto, C.; King, A.P.; Schnabel, J.A. Deep Learning-Based Detection and Correction of Cardiac MR Motion Artefacts During Reconstruction for High-Quality Segmentation. *IEEE Trans Med Imaging* **2020**, *39*, 4001–4010, doi:10.1109/TMI.2020.3008930.
38. Petersen, S.E.; Matthews, P.M.; Francis, J.M.; Robson, M.D.; Zemrak, F.; Boubertakh, R.; Young, A.A.; Hudson, S.; Weale, P.; Garratt, S.; et al. UK Biobank's Cardiovascular Magnetic Resonance Protocol. *Journal of Cardiovascular Magnetic Resonance* **2016**, *18*, 8, doi:10.1186/s12968-016-0227-4.
39. Bernard, O.; Lalande, A.; Zotti, C.; Cervenansky, F.; Yang, X.; Heng, P.-A.; Cetin, I.; Lekadir, K.; Camara, O.; Gonzalez Ballester, M.A.; et al. Deep Learning Techniques for Automatic MRI Cardiac Multi-Structures Segmentation and Diagnosis: Is the Problem Solved? *IEEE Transactions on Medical Imaging* **2018**, *37*, 2514–2525, doi:10.1109/TMI.2018.2837502.
40. Schär, M.; Kozerke, S.; Fischer, S.E.; Boesiger, P. Cardiac SSFP Imaging at 3 Tesla. *Magn Reson Med* **2004**, *51*, 799–806, doi:10.1002/mrm.20024.
41. Mueller, S.G.; Weiner, M.W.; Thal, L.J.; Petersen, R.C.; Jack, C.R.; Jagust, W.; Trojanowski, J.Q.; Toga, A.W.; Beckett, L. Ways toward an Early Diagnosis in Alzheimer's Disease: The Alzheimer's Disease Neuroimaging Initiative (ADNI). *Alzheimers Dement* **2005**, *1*, 55–66, doi:10.1016/j.jalz.2005.06.003.
42. Liu, W.; Wei, D.; Chen, Q.; Yang, W.; Meng, J.; Wu, G.; Bi, T.; Zhang, Q.; Zuo, X.-N.; Qiu, J. Longitudinal Test-Retest Neuroimaging Data from Healthy Young Adults in Southwest China. *Sci Data* **2017**, *4*, 170017, doi:10.1038/sdata.2017.17.
43. LaMontagne, P.J.; Benzinger, T.L.; Morris, J.C.; Keefe, S.; Hornbeck, R.; Xiong, C.; Grant, E.; Hassenstab, J.; Moulder, K.; Vlassenko, A.G.; et al. OASIS-3: Longitudinal Neuroimaging, Clinical, and Cognitive Dataset for Normal Aging and Alzheimer Disease 2019, 2019.12.13.19014902.
44. Sudlow, C.; Gallacher, J.; Allen, N.; Beral, V.; Burton, P.; Danesh, J.; Downey, P.; Elliott, P.; Green, J.; Landray, M.; et al. UK Biobank: An Open Access Resource for Identifying the Causes of a Wide Range of Complex Diseases of Middle and Old Age. *PLoS Med* **2015**, *12*, e1001779, doi:10.1371/journal.pmed.1001779.
45. Lebel, R.M. Performance Characterization of a Novel Deep Learning-Based MR Image Reconstruction Pipeline 2020.
46. Regulation (EU) 2016/679 of the European Parliament and of the Council of 27 April 2016 on the Protection of Natural Persons with Regard to the Processing of Personal Data and on the Free Movement of Such Data (General Data Protection Regulation) 2016.
47. Health Insurance Portability and Accountability Act of 1996 (HIPAA) 1996.